

# Plasminogen activator-coated nanobubbles targeting cell-bound $\beta$ 2-glycoprotein I as a novel thrombus-specific thrombolytic strategy

Paolo Macor,<sup>1</sup> Paolo Durigutto,<sup>2</sup> Monica Argenziano,<sup>3</sup> Kate Smith-Jackson,<sup>4</sup> Sara Capolla,<sup>5</sup> Valeria Di Leonardo,<sup>1</sup> Kevin Marchbank,<sup>4</sup> Valerio Stefano Tolva,<sup>6</sup> Fabrizio Semeraro,<sup>7</sup> Concetta T. Ammollo,<sup>7</sup> Mario Colucci,<sup>7</sup> Roberta Cavalli,<sup>3</sup> Pierluigi Meroni<sup>2</sup> and Francesco Tedesco<sup>2</sup>

<sup>1</sup>Department of Life Sciences, University of Trieste, Trieste, Italy; <sup>2</sup>Istituto Auxologico Italiano, IRCCS, Laboratory of Immuno-Rheumatology, Milan, Italy; <sup>3</sup>Department of Scienza e Tecnologia del Farmaco, University of Turin, Turin, Italy; <sup>4</sup>Translational and Clinical Research Institute, Faculty of Medical Sciences, Newcastle University, Newcastle, UK; <sup>5</sup>Experimental and Clinical Pharmacology Unit, C.R.O.-IRCCS, Aviano, Italy; <sup>6</sup>Struttura Complessa di Chirurgia Vascolare, ASST GOM Niguarda, Milano, Italy and <sup>7</sup>Dipartimento di Scienze Biomediche e Oncologia Umana, Università degli Studi di Bari Aldo Moro, Bari, Italy

**Correspondence:** P. Macor  
pmacor@units.it

**Received:** June 8, 2022.

**Accepted:** September 22, 2022.

**Early view:** September 29, 2022.

<https://doi.org/10.3324/haematol.2022.281505>

©2023 Ferrata Storti Foundation

Published under a CC BY-NC license 

## Abstract

$\beta$ 2-glycoprotein I ( $\beta$ 2-GPI) is a serum protein widely recognized as the main target of antibodies present in patients with antiphospholipid syndrome (APS).  $\beta$ 2-GPI binds to activated endothelial cells, platelets and leukocytes, key players in thrombus formation. We developed a new targeted thrombolytic agent consisting of nanobubbles (NB) coated with recombinant tissue plasminogen activator (rtPA) and a recombinant antibody specific for cell-bound  $\beta$ 2-GPI. The therapeutic efficacy of targeted NB was evaluated *in vitro*, using platelet-rich blood clots, and *in vivo* in three different animal models: i) thrombosis developed in a rat model of APS; ii) ferric chloride-induced mesenteric thrombosis in rats, and iii) thrombotic microangiopathy in a mouse model of atypical hemolytic uremic syndrome (C3-gain-of-function mice). Targeted NB bound preferentially to platelets and leukocytes within thrombi and to endothelial cells through  $\beta$ 2-GPI expressed on activated cells. *In vitro*, rtPA-targeted NB (rtPA-tNB) induced greater lysis of platelet-rich blood clots than untargeted NB. In a rat model of APS, administration of rtPA-tNB caused rapid dissolution of thrombi and, unlike soluble rtPA that induced transient thrombolysis, prevented new thrombus formation. In a rat model of ferric chloride triggered thrombosis, rtPA-tNB, but not untargeted NB and free rtPA, induced rapid and persistent recanalization of occluded vessels. Finally, treatment of C3-gain-of-function mice with rtPA-tNB, that target  $\beta$ 2-GPI deposited in kidney glomeruli, decreased fibrin deposition, and improved urinalysis data with a greater efficiency than untargeted NB. Our findings suggest that targeting cell-bound  $\beta$ 2-GPI may represent an efficient and thrombus-specific thrombolytic strategy in both APS-related and APS-unrelated thrombotic conditions.

## Introduction

Antiphospholipid syndrome (APS) is an autoimmune disease characterized by antibody-mediated vascular thrombosis and adverse pregnancy outcomes including fetal loss, pre-eclampsia, preterm delivery, and intrauterine growth restriction.<sup>1,2</sup> Vascular thrombosis is a serious and often recurrent medical condition that affects relatively young individuals with important social and clinical implications.<sup>3,4</sup> Vessel occlusion by blood clots is the most common clinical manifestation observed in a 10-year prospective study of 1,000 APS patients followed in various University Hospitals in Europe.<sup>5</sup> Although thrombi may potentially form in all arteries and veins of the vascular tree, clinical observation of APS patients has revealed 40%

localization in certain districts of the circulatory system, that are responsible for stroke, myocardial infarction, deep vein thrombosis, pulmonary embolism, and other less frequent vascular manifestations.<sup>5</sup>

Evidence collected from clinical studies and animal models of APS has documented the critical role played by antibodies to  $\beta$ 2-glycoprotein I ( $\beta$ 2-GPI) in thrombus formation. Medium-to-high-titer antibodies are detected in APS patients with increased risk of thrombosis and are listed among the classification criteria for the diagnosis of the disease.<sup>6</sup>  $\beta$ 2-GPI is a five-domain serum protein now recognized to be the main target of antiphospholipid antibodies. Four domains (DI-IV) are composed of short consensus repeats of approximately 60 amino acids shared with other members of the complement (C) con-

trol protein family, while the fifth domain contains a phospholipid binding site that interacts with the membrane of various cell types involved in thrombus formation including endothelial cells, platelets, and leukocytes.<sup>7,8</sup> The binding of  $\beta$ 2-GPI to endothelial cells requires cell priming with LPS, as documented by the analysis of the *in vivo* protein biodistribution in mice,<sup>9</sup> and may also be induced by pro-inflammatory and physical stimuli such as surgery.<sup>10</sup> An epitope exposed in the open form of  $\beta$ 2-GPI on the N-terminal DI is the preferential target of the pathogenic antibodies that induce thrombus formation.<sup>11</sup> The critical role played by the C system in this process is supported by the finding that vascular thrombosis, caused by passive administration of patients' antibodies or a monoclonal antibody to DI in an animal model of APS, is not observed in C-deficient animals or in animals receiving a non-C fixing antibody.<sup>11,12</sup> Despite the beneficial effect of long-term anticoagulation with vitamin K antagonists, recurrent thrombosis has been reported in 30-40% of high-risk patients with triple APL positivity<sup>5</sup> and remains a problem to be solved. Resolution of thrombi formed in carotid and cerebral arteries, and less frequently in coronary arteries, that cause serious clinical consequences including death, still represents an unmet clinical need. Thrombolytic agents administered to dissolve thrombi and surgical intervention aimed at removing blood clots in medium-large arteries in a limited number of patients unresponsive to pharmacologic treatment are the therapies currently used to control thrombosis in APS patients. However, despite the beneficial effect observed in patients treated with recombinant tissue plasminogen activator (rtPA), this therapy has significant limitations in safety and efficacy.<sup>13</sup> Bleeding is a serious side effect frequently observed in patients with ischemic stroke receiving rtPA and can be reduced, but not abolished, using a lower dose of the drug. Moreover, the rapid clearance of rtPA from the circulation, the relative resistance of large vessels to recanalization and the modest response observed in approximately 40% of patients with small vessel occlusions represent additional limitations of the thrombolytic therapy.<sup>14-16</sup>

The aim of this work was to devise a strategy to selectively deliver rtPA at sites of vessel-occluding thrombi in an attempt to reduce the systemic side effects of the thrombolytic therapy and to make the treatment more effective. The therapeutic approach was based on the administration of polymer-shelled nanobubbles (NB) conjugated with rtPA and a recombinant antibody specific for  $\beta$ 2-GPI bound to activated endothelial cells lining the occluded vessel, and to activated platelets and leukocytes that accumulate within the thrombus. Moreover, considering that  $\beta$ 2-GPI binds to these cells independently of antiphospholipid antibodies, we investigated whether this type of engineered NB had also a beneficial effect in thrombosis models unrelated to APS.

## Methods

### Nanobubbles preparation and characterization

NB with a perfluoropentane core and a chitosan shell were prepared by tuning a method previously reported<sup>17</sup> and used at the final concentration of  $4 \times 10^{11}$  NB/mL saline. Further details are available in the *Online Supplementary Appendix*.

### Patients' sera

Serum samples were obtained from five APS patients with medium-high titer antibodies to the DI domain of  $\beta$ 2-GPI after obtaining informed consent and were previously shown to induce clot formation in rats.<sup>18</sup> The ethical committee of Istituto Auxologico Italiano approved the study.

### Human thrombi

Three patients aged 60-72 years with clinical atherosclerotic disease, undergoing thrombectomy for thrombotic occlusion of descending thoracic aorta, popliteal or femoral arteries gave written informed consent to use surgically removed thrombi for research purposes. *In vitro* clots were prepared from freshly collected citrated human blood by the addition of thromboplastin and  $\text{CaCl}_2$ . Two different types of clots were generated: i) blood clots prepared under static conditions,<sup>19</sup> referred to as platelet-poor clots, and ii) blood clots prepared under flowing conditions (Chandler loop),<sup>20</sup> that have been shown to resemble arterial thrombi, and referred to as platelet-rich clots. Patient's thrombi and *in vitro*-generated clots (prepared from 3 different donors) were fixed for 24 hours in 10% buffered formalin, snap-frozen and embedded in OCT medium (Diagnostic Division; Miles Inc).

### Immunofluorescence analysis

Patients' thrombi, *in vitro* blood clots and kidneys from C3 gain-of-function (GOF) mice were examined by immunofluorescence as detailed in the *Online Supplementary Appendix*.

### *In vitro* fibrinolytic and thrombolytic assays

The fibrinolytic and thrombolytic activities of rtPA-coated NB were estimated as previously reported.<sup>20,21</sup> Further details are available in the *Online Supplementary Appendix*.

### Animal models

Experimental thrombosis models were established in male Wistar rats (270-290 g) kept under standard conditions in the Animal House of the University of Trieste, Italy, and in C3 GOF mice at Newcastle University, UK. The *in vivo* procedures were performed in compliance with the guidelines of European (86/609/EEC) and Italian (Legislative Decree 116/92) laws and were approved by the Italian Ministry of University and Research (Prot. N°

910/2018PR, rat models) and by the ethics committee of the Comparative Biology Center of Newcastle University (United Kingdom's Home Office granted license PD86B3678, mice model). The study was conducted in accordance with the Declaration of Helsinki.

### Antiphospholipid syndrome model

We used a previously published model of APS.<sup>12</sup> Further details are available in the *Online Supplementary Appendix*.

### Ferric chloride-induced thrombosis

The experiments were carried out according to Li *et al.*,<sup>22</sup> in anesthetized rats following an incision made through the abdominal wall to exteriorize the ileal mesentery.<sup>23</sup> Further details are available in the *Online Supplementary Appendix*.

### C3 gain-of-function mouse model of atypical hemolytic uremic syndrome

The C3 GOF mouse model of atypical hemolytic uremic syndrome (aHUS) has been previously published.<sup>24</sup> Further details are available in the *Online Supplementary Appendix*.

### Nanobubbles distribution in rat

*In vivo* biodistribution studies were performed in two anesthetized rats per group that received an intraperitoneal injection of LPS followed by either tNB conjugated with 3 nmol of cyanine 5.5 or saline and euthanized 2 hours later. The organs were analyzed *ex vivo* by IVIS Lumina III (PerkinElmer, Milan, Italy).<sup>25,26</sup>

### Statistical analysis

Data are presented as mean  $\pm$  standard deviation. Difference between groups was assessed by one-way analysis of variance (ANOVA) followed by Student-Newman-Keuls test for pairwise comparisons. Survival estimates were calculated according to Kaplan-Meier and compared with the log rank test. A two-sided *P* value of 0.05 was considered significant. Statistical analyses were done with GraphPad Prism 9 (San Diego, CA).

## Results

### Expression of $\beta$ 2-GPI on thrombi

In the initial experiments, we sought to determine whether  $\beta$ 2-GPI may represent a potentially valuable target for antibody-coated thrombolytic NB. For this purpose, we searched for the presence of  $\beta$ 2-GPI in the thrombi surgically removed from three patients with arterial thrombotic occlusions (Figure 1A) or *in vitro*-formed blood clots with different composition (Figure 1B). Staining of patient's

thrombus sections with antibodies to  $\beta$ 2-GPI and to either fibrin or CD9 (to detect platelets and leukocytes) revealed co-localization of  $\beta$ 2-GPI with platelets and leukocytes but not with fibrin. Deposits of  $\beta$ 2-GPI on nucleated cells were also observed by nuclear staining with DAPI (Figure 1A). The preferential deposition of  $\beta$ 2-GPI on platelets and nucleated cells was confirmed by the more intense staining of *in vitro* clots formed under flow conditions (Chandler thrombi), which resemble platelet-rich arterial thrombi, as compared to platelet-poor clots generated under static conditions (Figure 1B).

### Preparation and targeting properties of nanobubble formulations

A recombinant scFv-Fc miniantibody (MBB2) containing the hinge-CH2-CH3 domains of human IgG1 engineered from scFv isolated from phage display library was selected to functionalize the NB as ligand for bound  $\beta$ 2-GPI.<sup>11</sup> In order to avoid C activation by the MBB2/ $\beta$ 2-GPI complex, a CH2-deleted variant of MBB2 (MBB2 $\Delta$ CH2) was conjugated to NB via a covalent bond. Transmission electron microscopy (TEM) analysis of the NB showed no difference in the morphology of targeted and untargeted NB (Figure 2A). Likewise, the two types of NB had a similar size with an average diameter of  $363.5 \pm 10.6$  nm for the untargeted NB and  $359 \pm 12.5$  nm for the targeted NB and both the polydispersity index, a measure of particle size distribution, and the Z potential, an indicator of particle charge, were within the same range (Figure 2B).

Analysis of NB interaction with thrombi revealed a significant binding of MBB2 $\Delta$ CH2-coated NB that was inhibited by 10-fold excess soluble MBB2 $\Delta$ CH2, but not by an unrelated recombinant antibody,<sup>27,28</sup> preincubated with the clot section (Figure 2C), supporting the targeting specificity for  $\beta$ 2-GPI. Search for binding of tNB was extended to thrombi induced *in vivo* by patients' sera containing antibodies to  $\beta$ 2-GPI. Rhodamine 6G was administered to anesthetized rat to stain platelets and leukocytes prior to infusion of antibodies to  $\beta$ 2-GPI. Targeted or control NB loaded with coumarin 6 were infused immediately after formation of thrombi in mesenteric microvessels. Analysis of NB distribution in rats revealed selective co-localization of tNB and platelets/leukocytes in blood clots while untargeted NB were practically undetectable (Figure 2D; *Online Supplementary Videos S1 and S2*).

### Preparation and evaluation of *in vitro* thrombolytic activity of rtPA-coated nanobubbles

In order to selectively deliver the thrombolytic agent at site of thrombi and avoid its release into the circulation, rtPA was covalently conjugated to the NB shell exploiting two binding methods. The fibrinolytic activity of the two types of rtPA-coated NB was investigated by a turbidimetric clot lysis assay in which the NB were added to plasma

prior to clot formation. As shown in *Online Supplementary Figure S1*, type B rtPA-NB (carbodiimide-mediated amide bond) displayed a concentration-dependent fibrinolytic activity, which was comparable to that of soluble rtPA, whereas type A rtPA-NB (amino-reductive reaction) were inactive at all tested concentrations. Based on these results, type B rtPA-NBs coated with MBB2 $\Delta$ CH2 (rtPA-tNB) or untargeted (rtPA-NB) were used for all the *in vitro* and *in vivo* experiments.

The physico-chemical properties of rtPA-tNB, including the size, the polydispersity index and the Z potential, were essentially similar to those observed with rtPA-NB (Figure 3A). The encapsulation efficiency, expressed as percentage amount of rtPA loaded on NB / total amount of rtPA, was over 90% and the loading capacity, expressed as percentage amount of rtPA loaded / total weight of NB, was about 3.5%. These data did not change when rtPA was loaded on tNB. The amount of rtPA bound to NB stored at

4°C was quantified and functionally evaluated at different time points and found to be stable for up to 6 months.

The *in vitro* thrombolytic activity of targeted and untargeted rtPA-NB was investigated in a model consisting of platelet-rich blood clots bathed in autologous plasma. Upon addition of the fibrinolytic agent to the plasma surrounding the clot, the degree of lysis by targeted NB was greater than that of untargeted NB and was comparable to that of soluble rtPA (Figure 3B). The thrombolytic activity of untargeted rtPA-NB can be most likely attributed to the static conditions of the *in vitro* clot lysis and to the continued presence of the thrombolytic agent in the plasma surrounding the clot.

#### Effect of targeted nanobubbles on thrombi in the rat model of antiphospholipid syndrome

In order to investigate the thrombolytic effect of rtPA-tNB in the rat model of APS, NB were infused intravenously

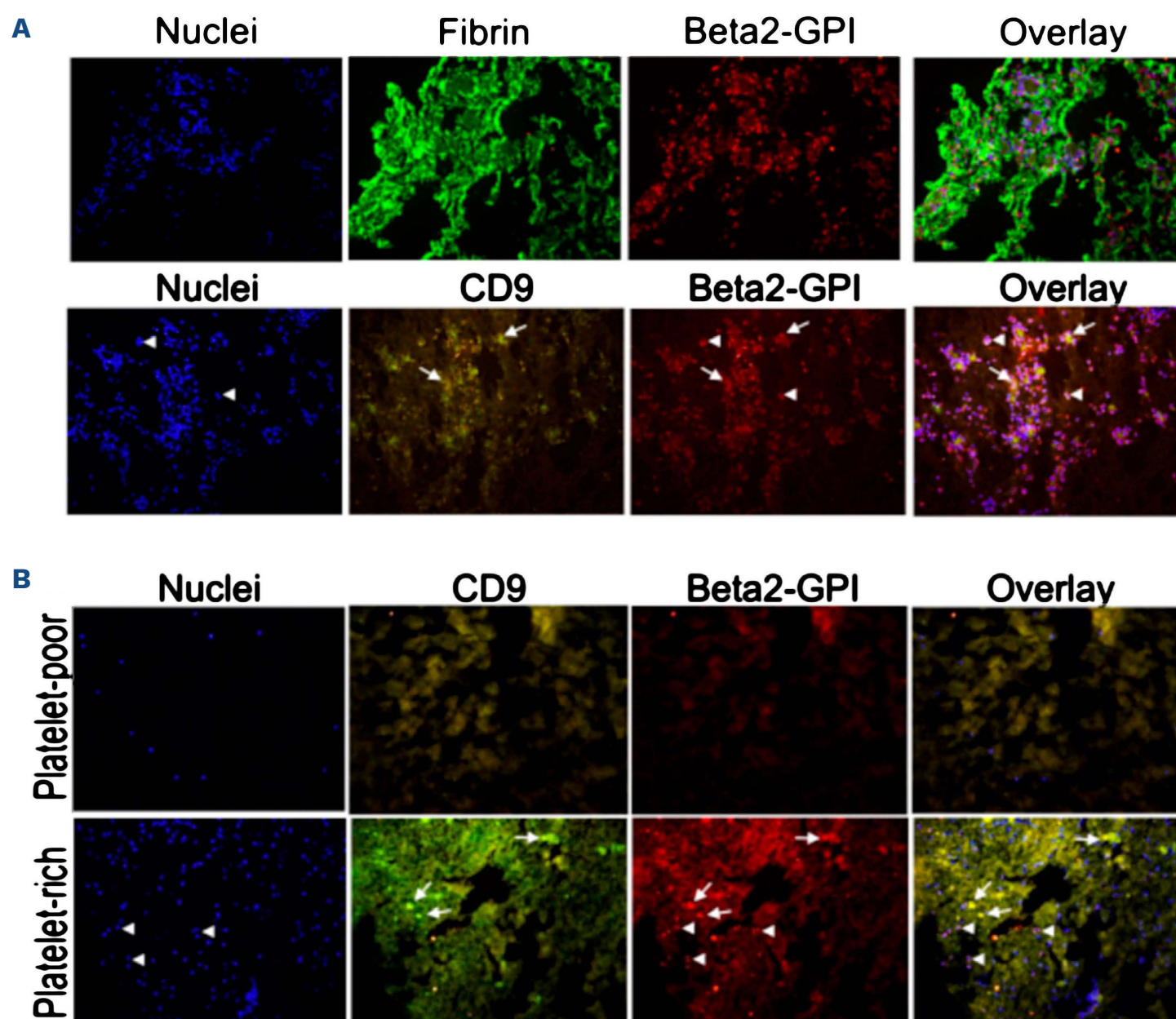


**Figure 1. Detection of  $\beta$ 2-GPI on thrombi by immunofluorescence analysis.** Clot sections were double stained with rabbit antibody to  $\beta$ 2 glycoprotein 1 ( $\beta$ 2-GPI) and either antibody to fibrin or to CD9, to investigate the localization of  $\beta$ 2-GPI on fibrin, platelets and leukocytes. DAPI was used to stain cell nuclei. The thrombi were obtained from 2 different sources: (A) 3 patients undergoing surgical thrombectomy; (B) *in vitro* blood clots generated under static (platelet-poor) or flow (platelet-rich) conditions (see Methods for additional details). Representative images of thrombus section from 1 patient showing absence of co-staining of  $\beta$ 2-GPI and fibrin. Arrows highlight the co-localization of  $\beta$ 2-GPI with CD9-positive structures and arrowheads show the co-localization of  $\beta$ 2-GPI with DAPI-positive nucleated cells.

after thrombus formation, approximately 30 minutes (min) after the injection of antibodies to  $\beta$ 2-GPI, and the presence and size of rhodamine 6G-stained thrombi in mesenteric vessels were monitored over time. Administration of rtPA-tNB caused thrombolysis within 1 min (*Online Supplementary Video S3*) as opposed to the less rapid dissolution of thrombi caused by soluble rtPA (*Online Supplementary Video S4*), whereas untargeted rtPA-NB were ineffective (*Online Supplementary Video S5*). The dissolution of the thrombi, obtained with rtPA-tNB and soluble rtPA, was confirmed by quantitative analysis of rhodamine 6G intensity staining (Figure 4A). A point to emphasize is that the dose of rtPA bound to NB was 10 times lower than that of the soluble rtPA. Moreover, as shown in Figure 4A and *Online Supplementary Video S3* and *S4*, sol-

uble rtPA exhibited a transient thrombolytic effect that lasted less than 3 min and was followed by the formation of new thrombi. Conversely, rtPA-tNB induced fast thrombolysis and prevented the formation of new thrombi during the 90-minute observation period (Figure 4A). Untargeted rtPA-NB failed to lyse the thrombi at all time points (Figure 4A; *Online Supplementary Video S5*). We further analyzed the efficacy of rtPA-tNB on blood vessels occlusion by evaluating the number of vessels with markedly reduced or absent blood flow. The results presented in Figure 4B show that treatment with rtPA-tNB resulted in vascular recanalization and restoration of blood flow in over 80% of occluded vessels whereas both rtPA and rtPA-NB were ineffective.

The endothelium of the mesenteric vessels examined at

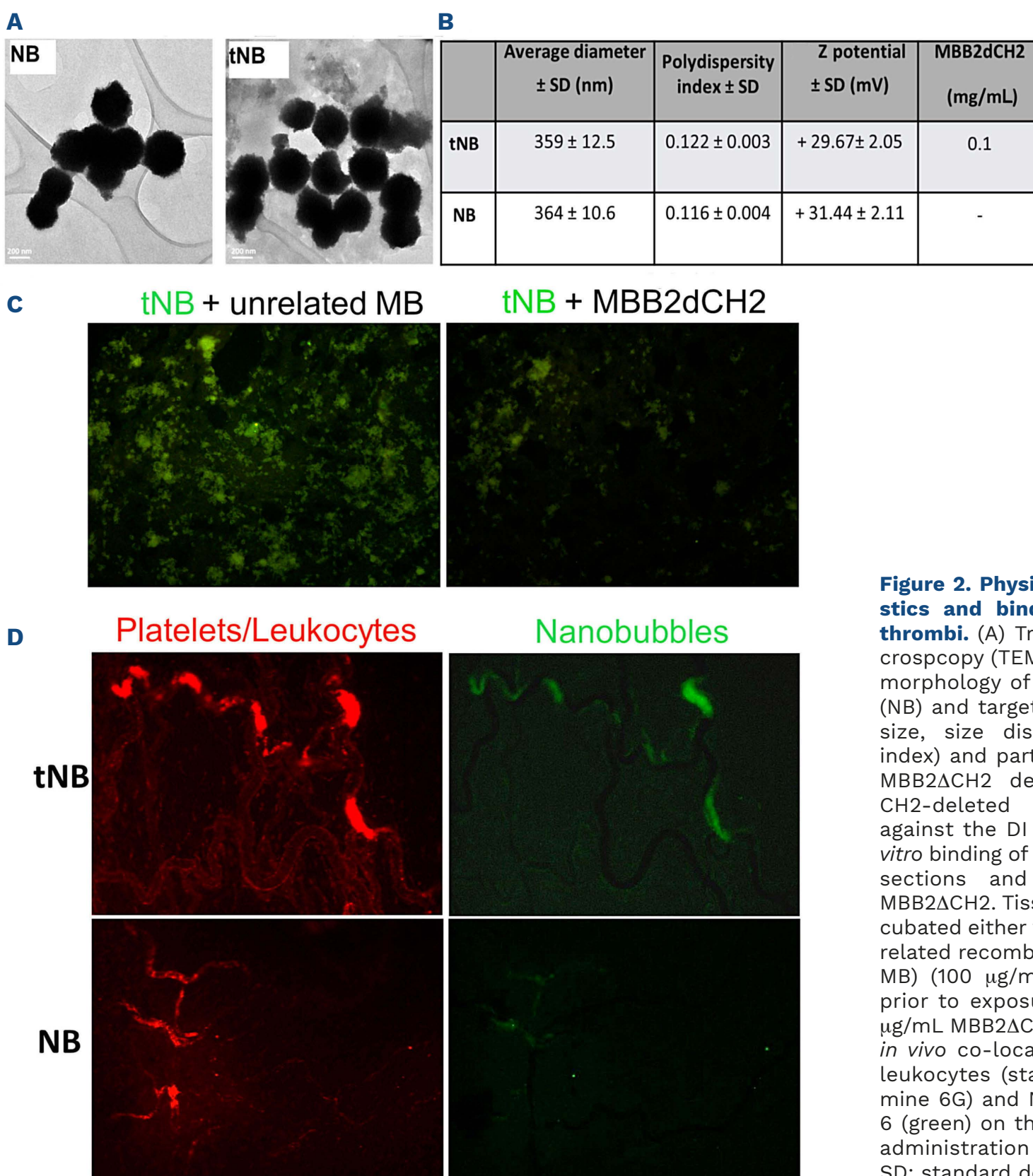


**Figure 2. Physico-chemical characteristics and binding of nanobubbles to thrombi.** (A) Transmission electron microscopy (TEM) images showing similar morphology of untargeted nanobubbles (NB) and targeted NB (tNB); (B) average size, size distribution (polydispersity index) and particle charge (Z potential); MBB2 $\Delta$ CH2 denotes the recombinant CH2-deleted scFv-Fc miniantibody against the D1 domain of  $\beta$ 2-GPI. (C) *In vitro* binding of tNB to patient's thrombus sections and inhibition by soluble MBB2 $\Delta$ CH2. Tissue sections were pre-incubated either with MBB2 $\Delta$ CH2 or an unrelated recombinant antibody (unrelated MB) (100  $\mu$ g/mL) for 15 minutes (min) prior to exposure to tNB containing 10  $\mu$ g/mL MBB2 $\Delta$ CH2 for further 60 min; (D) *In vivo* co-localization of platelets and leukocytes (stained in red with rhodamine 6G) and NB loaded with coumarin 6 (green) on thrombi induced in rats by administration of antibodies to  $\beta$ 2-GPI. SD: standard deviation.

the end of the experiment was still covered by tNB indicating a stable interaction of  $\beta$ 2-GPI with endothelial cells (Figure 5). This finding might explain the prolonged profibrinolytic effect observed after administration of rtPA-tNB. No sign of vascular leakage, assessed by extravascular diffusion of free rhodamine 6G, or blood extravasation was seen in the ileal mesentery of rats treated with rtPA-tNB throughout the experimental procedure despite the micro-traumas caused by the tissue manipulation during the mesentery exteriorization from the abdominal cavity to petri dishes for the intravital microscopy analysis. It is important to underline that only a small percentage of the infused tNB localized in the thrombi while a large proportion was cleared by the liver and, to a lesser extent, by the lung (*Online Supplementary Figure S2*).

### Effect of targeted nanobubbles on ferric chloride thrombosis

Having found that  $\beta$ 2-GPI was expressed on thrombi independently of the presence of antibodies to this protein, we sought to determine whether rtPA-tNB may also be effective in lysing blood clots induced by ferric chloride ( $\text{FeCl}_3$ ) applied to the rat mesentery. As in the case of APS, the NB were infused soon after thrombus formation, which occurred within 10 min after removal of the chemical compound applied to the mesentery. Unlike rtPA and untargeted NB, rtPA-tNB localized at the thrombus site (Figure 6A) and induced rapid and persistent thrombolysis (*Online Supplementary Video S6 to S8*). The greater effi-

cacy of rtPA-tNB was also confirmed by the substantial decrease in the percentage of occluded vessels that was not seen using either soluble rtPA or untargeted rtPA-NB (Figure 6B).

### Effect of targeted nanobubbles on the C3 gain-of-function murine model of atypical hemolytic uremic syndrome

Immunofluorescence analysis confirmed that both  $\beta$ 2-GPI and fibrin were co-localized within the glomeruli and renal vessels (*Online Supplementary Figure S3*), thus proving the rationale to test the *in vivo* therapeutic effect of rtPA-tNB. Mice exhibiting active disease (evidenced through an active urinary sediment) were randomized into three groups receiving saline, rtPA-NB or rtPA-tNB. As predicted, a modest reduction in fibrin deposition with rtPA-NB treatment was observed due to the thrombolytic effects of rtPA. However, rtPA-tNB, which enabled targeted therapy due to the addition of antibodies to  $\beta$ 2-GPI, significantly attenuated fibrin deposition within the glomeruli when compared to untreated animals and rtPA-NB-treated animals (Figure 7A and B).

Survival analysis showed that C3 GOF mice treated with rtPA-tNB had reduced mortality in comparison to saline-treated or rtPA-NB-treated animals (*Online Supplementary Figure S4A*); the difference, however, did not reach statistical significance because of the small number of animals. Urinalysis data are shown in the *Online Supplementary Figure S4B to D*. Saline group exhibit persisting hematuria,

**A**

Sample	Average diameter $\pm$ SD (nm)	PDI $\pm$ SD	Z potential $\pm$ SD (mV)	NB concentration ( $10^{11}$ /mL)	MBB2dCH2 (mg/mL)	rtPA (mg/mL)
rtPA-tNB	356.7 $\pm$ 9.5	0.123 $\pm$ 0.003	+ 28.65 $\pm$ 1.22	4	0.1	0.1
rtPA-NB	360.2 $\pm$ 12.3	0.125 $\pm$ 0.002	+ 29.03 $\pm$ 0.87	4,1	-	0.1

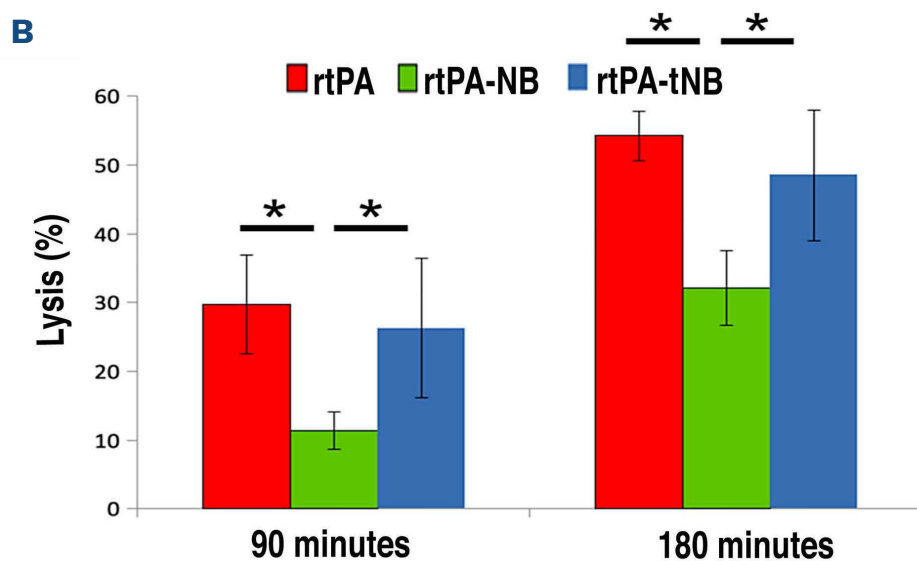


**Figure 3. Physico-chemical characteristics and functional activity of nanobubbles coated with recombinant tissue plasminogen activator.** (A) Size and characteristics of rtPA-tNB and rtPA-NB (see legend of Figure 2 for further details). (B) Thrombolytic activity of recombinant tissue plasminogen activator-bound (rtPA-bound) nanobubbles (NB) and soluble rtPA on blood clot formed under flow conditions (Chandler loop). NB (500 ng/mL bound rtPA) and soluble rtPA (500 ng/mL) were added to the plasma surrounding the clot and the percent lysis was determined at the indicated intervals as detailed in the Methods. The results are presented as mean  $\pm$  standard deviation (SD) of 3 different experiments. \* $P < 0.05$  using one-way ANOVA followed by Student-Newman-Keuls test.

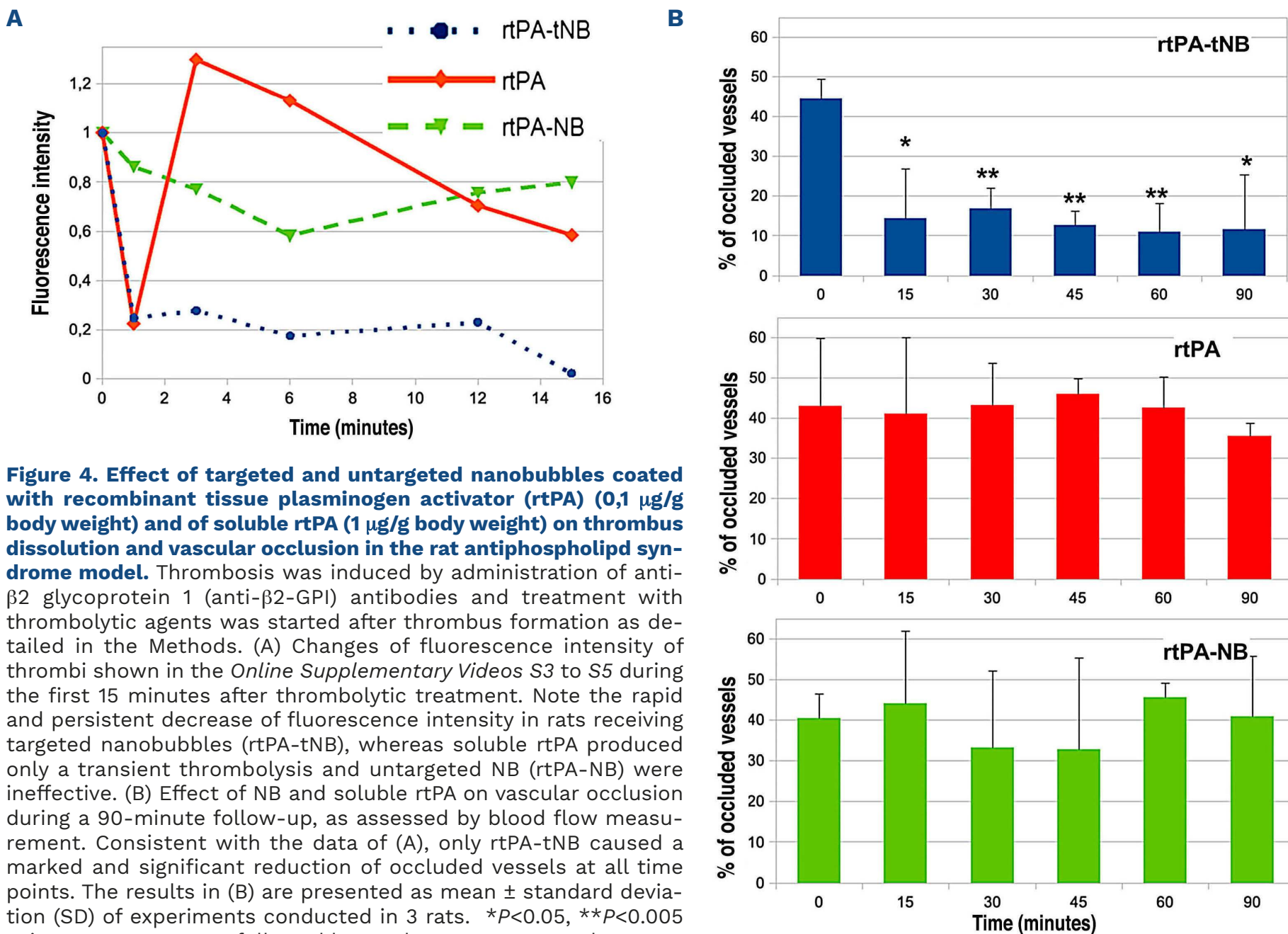


**Figure 4. Effect of targeted and untargeted nanobubbles coated with recombinant tissue plasminogen activator (rtPA) (0,1  $\mu$ g/g body weight) and of soluble rtPA (1  $\mu$ g/g body weight) on thrombus dissolution and vascular occlusion in the rat antiphospholipid syndrome model.** Thrombosis was induced by administration of anti- $\beta$ 2 glycoprotein 1 (anti- $\beta$ 2-GPI) antibodies and treatment with thrombolytic agents was started after thrombus formation as detailed in the Methods. (A) Changes of fluorescence intensity of thrombi shown in the *Online Supplementary Videos S3 to S5* during the first 15 minutes after thrombolytic treatment. Note the rapid and persistent decrease of fluorescence intensity in rats receiving targeted nanobubbles (rtPA-tNB), whereas soluble rtPA produced only a transient thrombolysis and untargeted NB (rtPA-NB) were ineffective. (B) Effect of NB and soluble rtPA on vascular occlusion during a 90-minute follow-up, as assessed by blood flow measurement. Consistent with the data of (A), only rtPA-tNB caused a marked and significant reduction of occluded vessels at all time points. The results in (B) are presented as mean  $\pm$  standard deviation (SD) of experiments conducted in 3 rats. \* $P < 0.05$ , \*\* $P < 0.005$  using one-way ANOVA followed by Student-Newman-Keuls test.

which reached clinical end point in five of six mice (*Online Supplementary Figure S4D*). In contrast, three of the five animals receiving rtPA-tNB showed improvement in hematuria after the second dose of the thrombolytic agent.

## Discussion

Nanoparticles are being developed as a novel therapeutic tool to deliver a sufficient amount of thrombolytic drugs to vessel-occluding thrombi and to reduce and possibly avoid serious side effects associated with the administration of soluble drugs. This therapeutic approach can be made more effective by coating NB with ligands that bind with reasonably good affinity to target molecules expressed on blood clots. The data presented here provide evidence that rtPA-coated NB targeting cell-bound  $\beta$ 2-GPI clear occluded vessels and re-establish blood flow in APS and non-APS thrombosis models.

Chitosan-shelled NB employed in this study have been largely used thanks to their stability, biocompatibility, low immunogenicity and biodegradability and have been

adopted in different biomedical and pharmaceutical fields.<sup>29,30</sup> The good biocompatibility of NB is related to their components, such as chitosan and phospholipids, that are biodegradable, safe and admitted by the Regulatory Agencies Food and Drug Administration and European Medicines Agency. Indeed, chitosan-shelled NB have previously been shown to be non-cytotoxic on different cell lines and no signs of acute toxicity was observed after intravenous or intradermal administration in animal models.<sup>31-33</sup> The approximately 400 nm size of the NB has the advantage of preventing or markedly reducing their renal excretion and their distribution is favored by the physical property of soft particles.<sup>34</sup> An additional advantage of the polymer-shelled NB is to be easily modified by covalently binding antibodies, aptamers, peptides and small molecules that allow selective *in vivo* localization.<sup>33,35</sup> Equally important is the characteristic of the NB to be filled with safe and biologically inert gases or vaporizable compounds such as perfluorocarbons, sulfur hexafluoride, air and carbon dioxide, enabling them to be good ultrasound reflectors and to be used as an ultrasound imaging probe to localize thrombi and monitor their *in vivo* dissolution.<sup>36</sup>

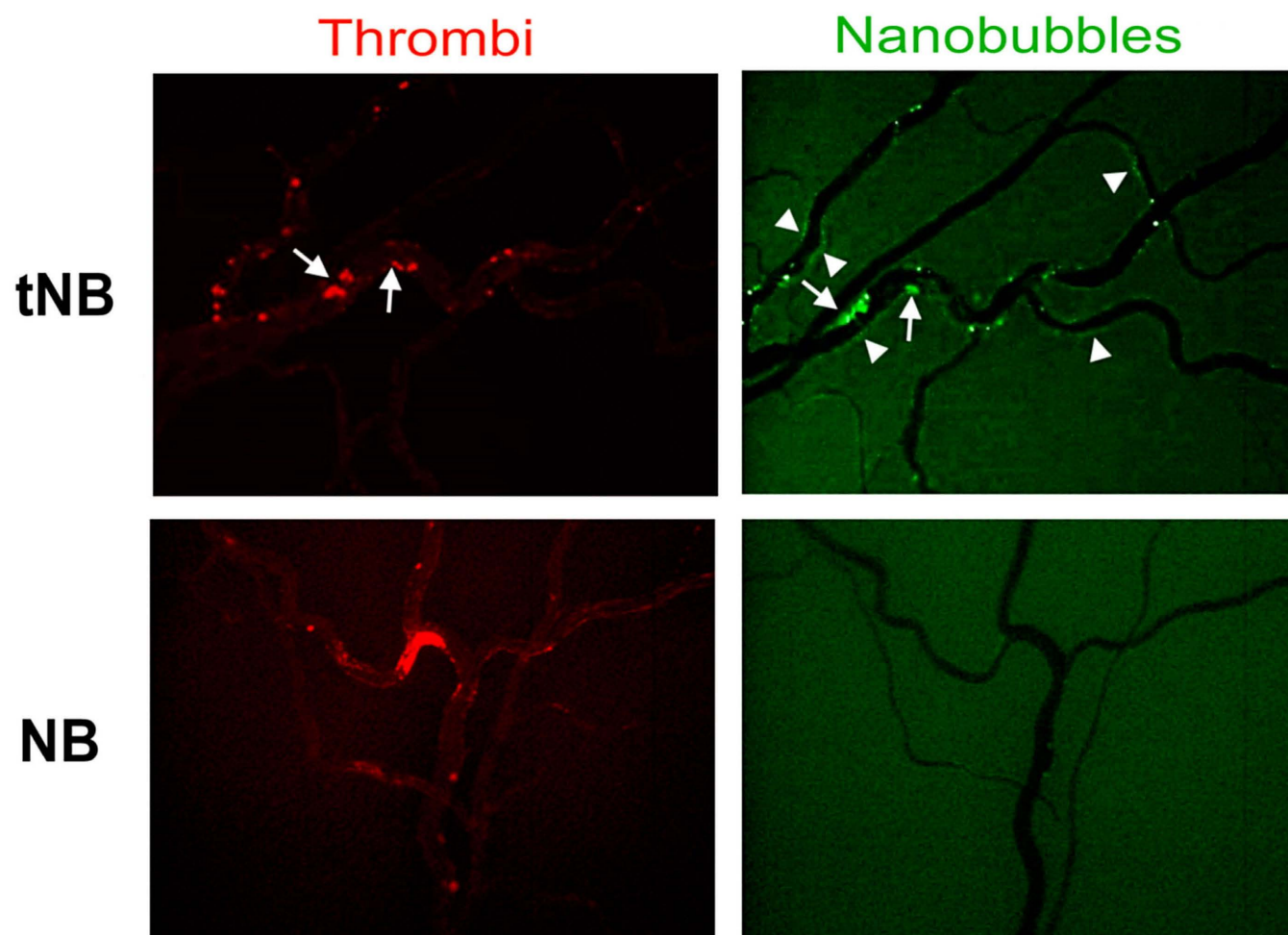


**Figure 5. Localization of targeted nanobubbles on endothelium and vascular thrombi during thrombolytic treatment in a rat model of antiphospholipid syndrome.** Thrombus formation and nanobubble (NB) deposits were followed by intravital microscopy and the images were collected 90 minutes after injection of NB. Residual intravascular thrombi are visualized in red by *in vivo* staining with rhodamine 6G and NB loaded with coumarin 6 in green. Arrows show the co-localization of rtPA-tNB and residual vascular thrombi and arrowheads highlight the localization of rtPA-tNB on activated endothelium. Note the absence of untargeted NB and the presence of occluded vessels in rtPA-NB-treated animal. TNB: targeted NB; rtPA: recombinant tissue plasminogen activator.

Platelets and fibrin, being the major components of vascular thrombi, have been investigated as potential targets for the local delivery of nanoparticles coated with thrombolytic agents. Monoclonal antibodies and peptides reacting with fibrin have proven successful for the selective delivery of nanoparticles to thrombi for theranostic purposes.<sup>37,38</sup> Satisfactory results have also been obtained targeting the platelets with a monoclonal antibody to the GPIIb/IIIa receptor expressed on both quiescent and activated platelets.<sup>39</sup> Unfortunately, treatment with this antibody is often associated with bleeding, which can be markedly reduced by targeting the platelets with a single-chain fragment variable that binds the activated form of GPIIb/IIIa.<sup>40</sup> Thrombus dissolution with minimal hemorrhagic risk has also been induced by microbubbles loaded with thrombolytic agents and targeted to blood clots by the arginine-glycine-aspartic acid-serine peptide.<sup>41</sup> However, this therapeutic approach has the limitation of having been tested on thrombi induced by either chemical or physical vascular injury, but not in models relevant to human diseases. We addressed this issue by selecting  $\beta$ 2-GPI as a target for the delivery of rtPA-coated NB to APS and non-APS thrombi. The advantage of  $\beta$ 2-GPI over other targets is to interact with different cells involved in throm-

bus formation including platelets, endothelial cells and leukocytes. These cells express several receptors for  $\beta$ 2-GPI such as ApoER2, Toll-like receptors 2 and 4, annexin A2, glycoprotein Iba, and LRP8,<sup>42</sup> though their *in vivo* relevance in the procoagulant effect of anti- $\beta$ 2-GPI antibodies in APS patients remains to be established. The endothelium is an important target of  $\beta$ 2-GPI and represents the initial site of clot formation triggered by the interaction of antibodies with cell-bound  $\beta$ 2-GPI. It is important to emphasize that binding of  $\beta$ 2-GPI to endothelial cells requires cell activation by LPS and possibly proinflammatory cytokines, and is independent of antibodies.<sup>9</sup> This is consistent with the finding reported here that  $\beta$ 2-GPI is localized on both renal vascular endothelium and glomeruli of a mouse model of aHUS in the absence of specific antibodies. Activation seems to be also required for the binding of  $\beta$ 2-GPI to platelets, as suggested by the detection of this molecule on platelets incubated with thrombin receptor-activating peptide, but not on resting platelets.<sup>43</sup> This observation is supported by our data showing that  $\beta$ 2-GPI is expressed in platelet-rich thrombi such as human arterial thrombi or *in vitro* formed platelet-rich blood clots (Chandler thrombi). However, platelets do not seem to be the only target of  $\beta$ 2-GPI

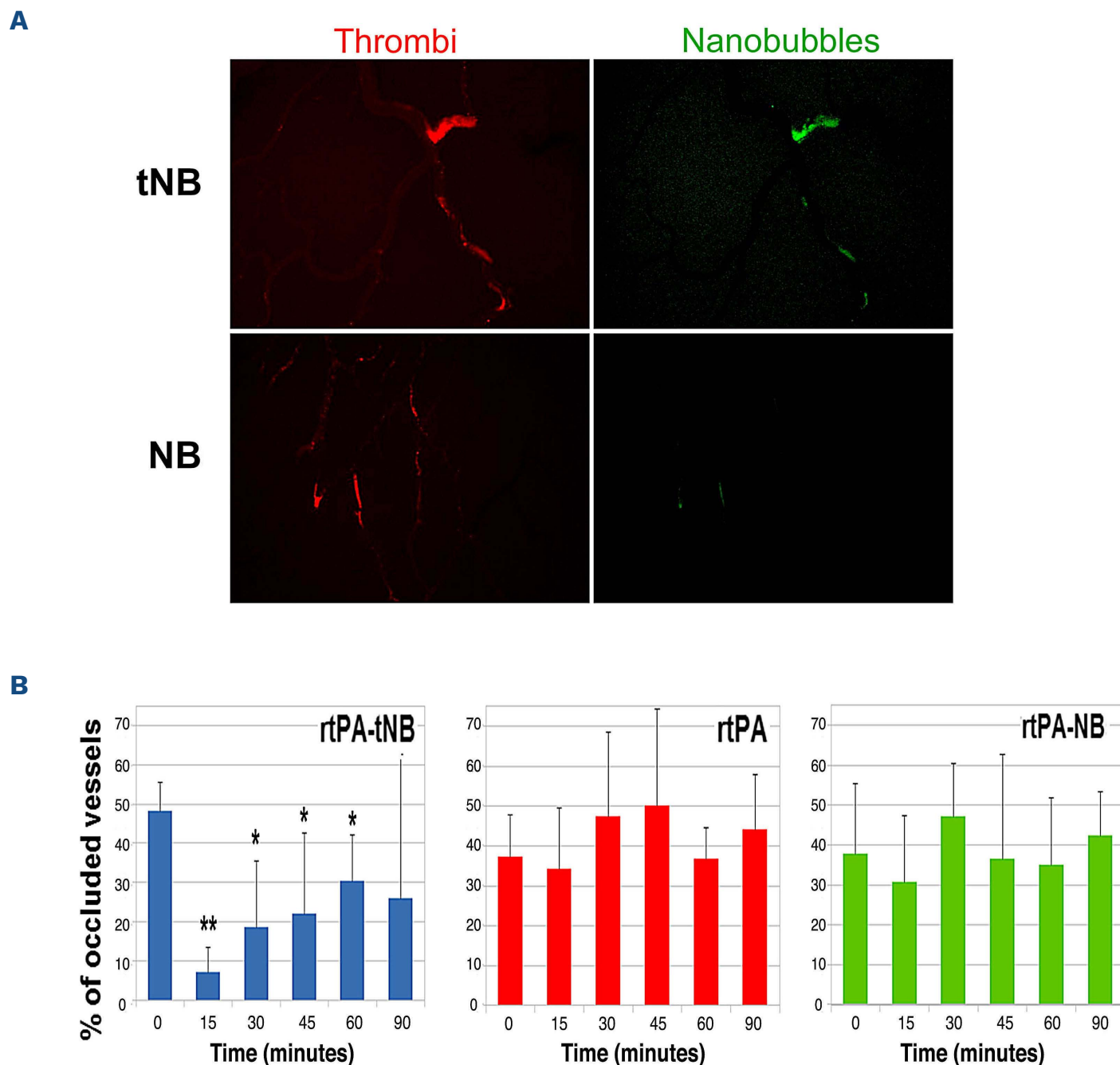


**Figure 6. Localization of targeted and untargeted nanobubbles (tNB and NB) (without recombinant tissue plasminogen activator [rtPA]) on vascular thrombi induced by ferric chloride and effect of rtPA-NB, rtPA-tNB and soluble rtPA on vascular thrombotic occlusion.** (A) Intravascular thrombi are visualized in red by *in vivo* staining with rhodamine 6G and in green by coumarin 6-loaded targeted nanobubbles (tNB). The images were collected 30 minutes after injection of NB. Note the absence of thrombus green staining in rats that received untargeted NB. (B) Time course of vascular occlusion after treatment with rtPA-coated tNB or untargeted NB (0,2  $\mu$ g/g body weight) or soluble recombinant tissue plasminogen activator (rtPA) (2  $\mu$ g/g body weight), as assessed by intravascular microscopy analysis. A significant reduction in the number of occluded vessels was seen in rats treated with targeted NB (rtPA-tNB) but not in those treated with untargeted NB or soluble rtPA. The results are presented as mean  $\pm$  standard deviation of experiments conducted in 3 rats. \* $P$ <0.05, \*\* $P$ < 0.005 using one-way ANOVA followed by Student-Newman-Keuls test.

in thrombi as positive staining was seen in thrombus-associated nucleated cells, which include monocytes and neutrophils, known to be involved in thrombogenesis by expressing and/or releasing tissue factor and neutrophil extracellular traps.<sup>44</sup>

The rtPA-coated tNB induced faster dissolution (within 1 min) of thrombi in the mesenteric microcirculation in the rat model of APS than soluble rtPA, whereas untargeted rtPA-NB were ineffective. These results clearly indicate that targeted NB are able to deliver rtPA to blood clots localized in large arteries as well as in microvessels of various organs observed in the classic APS, and in the more severe catastrophic APS. The *in vivo* effect of rtPA was transient because rethrombosis occurred within a few min and

persisted for the whole observation period. On the contrary, administration of targeted NB prevented the formation of new thrombi despite the presence of circulating thrombus-inducing antibodies to  $\beta$ 2-GPI. This protection against rethrombosis is most likely due to the binding of rtPA-bearing tNB to  $\beta$ 2-GPI deposited on the endothelium at sites of vascular thrombi, thereby creating a profibrinolytic shield. Moreover, the fast and persistent recanalization of occluded vessels by targeted NB was achieved with a dose of rtPA that was 10-fold lower than that of soluble rtPA, which is expected to significantly reduce the bleeding risk as suggested by our failure to detect bleeding in the ileal mesentery during the *in vivo* experiments. This greater efficiency can be explained by the reduced dispersion and the selec-

tive delivery of the thrombolytic agent bound to NB at sites of thrombus formation. One possible indication of this therapeutic approach in the clinical setting might be APS patients undergoing vascular surgery, who are known to be at high risk of rethrombosis as a result of  $\beta$ 2-GPI deposition on activated endothelium followed by the binding of pathogenic antibodies and C activation.<sup>10</sup>

Another important finding of this work is the ability of targeted NB to lyse thrombi in non-APS models such as ferric chloride-induced thrombosis<sup>45-47</sup> and the more clinically relevant atypical hemolytic uremic syndrome in C3 GOF mice that manifests with hematuria, proteinuria, high creatinine level, hemolysis, fibrin deposition in the glomeruli and occasional intravascular thromboses. As anticipated by our previous observations that chemical and physical stimuli can promote  $\beta$ 2-GPI deposition on endothelial cells,<sup>10,12</sup> it was not surprising to discover that the tNB were able to dissolve blood clots formed in vessels where the local application of ferric chloride leads to activation of endothelial cells and binding of  $\beta$ 2-GPI. Our data also show that thrombotic microangiopathy (TMA) observed in the C3 GOF mouse model of aHUS is a predisposing condition for the deposition of  $\beta$ 2-GPI on endothelial cells of glomeruli. The role of bound  $\beta$ 2-GPI is to focalize the delivery of rtPA-coated NB at sites of fibrin clots where they induce fibrin dissolution. The successful reduction of fibrin deposition within the microvasculature of the glomeruli in C3 GOF mice suggests this therapy could be a useful adjunct in the treatment of thrombotic microangiopathies. For C-mediated TMA, a C-inhibiting therapy will still be required to extinguish the disease process through restoring C regulation. However, restoration of C regulation takes time and thus a fast-acting prophylactic treatment with targeted fibrinolytic NB could reduce the fibrin burden within the glomeruli, thereby attenuating renal ischemic injury and thus end organ damage. This targeted therapy could be extended to patients with secondary TMA to reduce ischemic injury in the interim, whilst the precipitating factor of the TMA is identified and subsequently removed. Collectively, any reduction in end organ damage will translate to improved clinical outcomes.

In conclusion, rtPA-coated polymer-shelled NB targeted to  $\beta$ 2-GPI expressed on activated endothelial cells, platelets and leukocytes have been shown to be effective in dissolving thrombi and prevent rethrombosis in rat models of APS and ferric chloride thrombosis, as well as in removing fibrin deposits in the kidneys of mice that develop aHUS. Targeting cell-bound  $\beta$ 2-GPI may represent an efficient and safe strategy to selectively deliver a fibrinolytic agent at sites of thrombotic vessel occlusion as well as at sites at risk of developing thrombosis such as injured vascular districts, where activated endothelial cells, along with activated platelets and leukocytes adhering to their surface, might promote a strong thrombogenic environment.

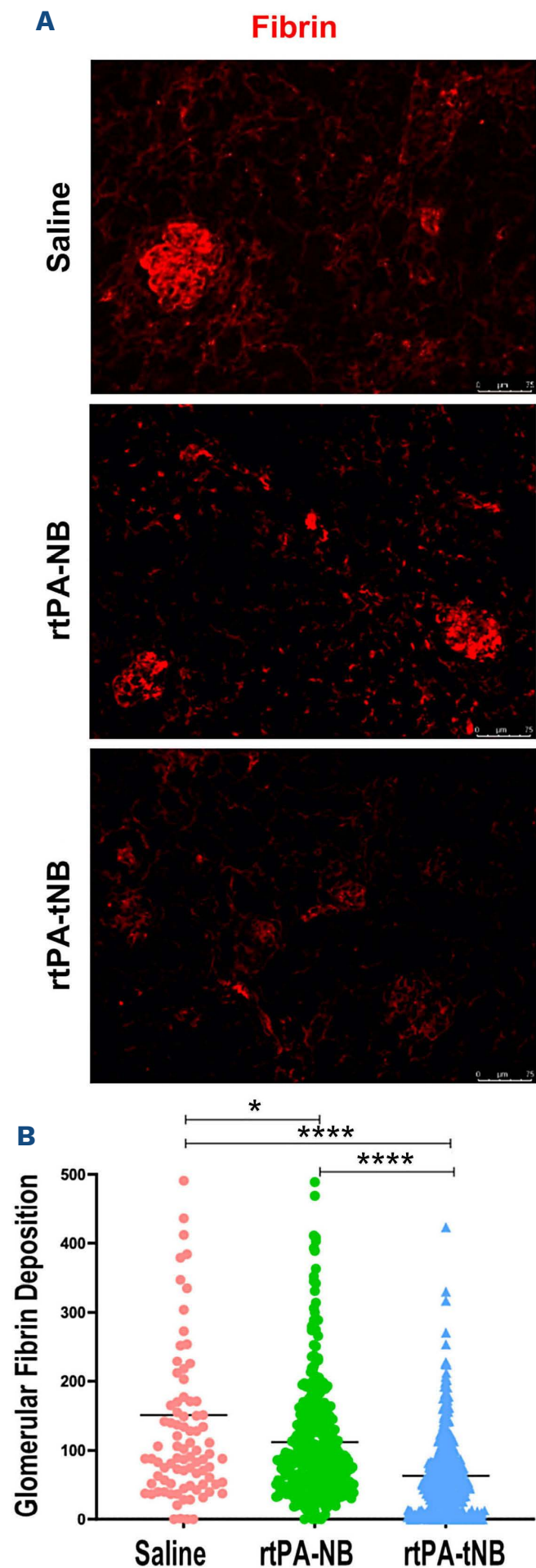


**Figure 7. Recombinant tissue plasminogen activator targeted nanobubbles dissolve clots in the C3 gain-of function mouse model of atypical hemolytic uremic syndrome.** (A) Representative image of glomerular fibrin deposition in saline-treated atypical hemolytic uremic syndrome (aHUS) mice (n=3), aHUS mice treated with rtPA-NB, (0,5  $\mu$ g/g body weight; n=6) or aHUS mice treated with recombinant tissue plasminogen activator targeted nanobubbles (rtPA-tNB) (0,5  $\mu$ g/g body weight; n=5). (B) Densitometry analysis of glomerular fibrin deposition, 87 glomeruli scored in saline-treated C3 gain of function (GOF), 358 glomeruli scored in rtPA-NB, 459 scored in rtPA-tNB. \* $P$ <0.05, \*\* $P$ <0.005, \*\*\* $P$ <0.0001 using one-way ANOVA followed by Student-Newman-Keuls test.

**Disclosures**

No conflicts of interest to disclose

**Contributions**

PM, RC, PLM, MC and FT designed the study. MA prepared and characterized the nanobubbles. PD, VDL, KM, SC and K S-J performed the *in vivo* experiments and analyzed the data. FS and CTA performed the *in vitro* fibrinolytic and thrombolytic assays and analyzed the data. VST surgically removed the thrombi from patients. FT and PM wrote the draft of the manuscript. RC, MC, PLM, KM and K S-J revised the manuscript.

**Funding**

This work was supported by funds from University of Trieste (to PM) and University of Turin (60% to MA and RC). KSJ is a Medical Research Council (MRC) clinical Fellow (MR/R001359/1). The paper was also supported in part by Ricerca Corrente 2019 and 2020 - Ministero della Salute, Italy (to PLM).

**Data-sharing statement**

All the data obtained in this study have been included in the article and the Online Supplementary Appendix and are available upon request to the corresponding author.

**References**

1. Meroni PL, Borghi MO, Grossi C, Chighizola CB, Durigutto P, Tedesco F. Obstetric and vascular antiphospholipid syndrome: same antibodies but different diseases? *Nat Rev Rheumatol*. 2018;14(7):433-440.
2. Meroni PL, Borghi MO, Raschi E, Tedesco F. Pathogenesis of antiphospholipid syndrome: understanding the antibodies. *Nat Rev Rheumatol*. 2011;7(6):330-339.
3. Garcia D, Erkan D. Diagnosis and management of the antiphospholipid syndrome. *N Engl J Med*. 2018;379(13):1290-1291.
4. Sciascia S, Sanna G, Murru V, Roccatello D, Khamashta MA, Bertolaccini ML. The global anti-phospholipid syndrome score in primary APS. *Rheumatology (Oxford)*. 2015;54(1):134-138.
5. Cervera R, Serrano R, Pons-Estel GJ, et al. Morbidity and mortality in the antiphospholipid syndrome during a 10-year period: a multicentre prospective study of 1000 patients. *Ann Rheum Dis*. 2015;74(6):1011-1018.
6. Miyakis S, Lockshin MD, Atsumi T, et al. International consensus statement on an update of the classification criteria for definite antiphospholipid syndrome (APS). *J Thromb Haemost*. 2006;4(2):295-306.
7. de Groot PG, Urbanus RT. The significance of autoantibodies against beta2-glycoprotein I. *Blood*. 2012;120(2):266-274.
8. Giannakopoulos B, Krilis SA. The pathogenesis of the antiphospholipid syndrome. *N Engl J Med*. 2013;368(11):1033-1044.
9. Agostinis C, Biffi S, Garrovo C, et al. In vivo distribution of beta2 glycoprotein I under various pathophysiologic conditions. *Blood*. 2011;118(15):4231-4238.
10. Meroni PL, Macor P, Durigutto P, et al. Complement activation in antiphospholipid syndrome and its inhibition to prevent rethrombosis after arterial surgery. *Blood*. 2016;127(3):365-367.
11. Agostinis C, Durigutto P, Sblattero D, et al. A non-complement-fixing antibody to beta2 glycoprotein I as a novel therapy for antiphospholipid syndrome. *Blood*. 2014;123(22):3478-3487.
12. Fischetti F, Durigutto P, Pellis V, et al. Thrombus formation induced by antibodies to beta2-glycoprotein I is complement dependent and requires a priming factor. *Blood*. 2005;106(7):2340-2346.
13. Thiebaut AM, Gauberti M, Ali C, et al. The role of plasminogen activators in stroke treatment: fibrinolysis and beyond. *Lancet Neurol*. 2018;17(12):1121-1132.
14. Campbell BC. Thrombolysis and thrombectomy for acute ischemic stroke: strengths and synergies. *Semin Thromb Hemost*. 2017;43(2):185-190.
15. Rabinstein AA. Update on treatment of acute ischemic stroke. *Continuum (Minneapolis)*. 2020;26(2):268-286.
16. Waqas M, Kuo CC, Dossani RH, et al. Mechanical thrombectomy versus intravenous thrombolysis for distal large-vessel occlusion: a systematic review and meta-analysis of observational studies. *Neurosurg Focus*. 2021;51(1):E5.
17. Cavalli R, Bisazza A, Trotta M, et al. New chitosan nanobubbles for ultrasound-mediated gene delivery: preparation and *in vitro* characterization. *Int J Nanomedicine*. 2012;7(1):3309-3318.
18. Durigutto P, Grossi C, Borghi MO, et al. New insight into antiphospholipid syndrome: antibodies to beta2glycoprotein I-domain 5 fail to induce thrombi in rats. *Haematologica*. 2019;104(4):819-826.
19. Colucci M, Scopece S, Gelato AV, Dimonte D, Semeraro N. In vitro clot lysis as a potential indicator of thrombus resistance to fibrinolysis - study in healthy subjects and correlation with blood fibrinolytic parameters. *Thromb Haemost*. 1997;77(4):725-729.
20. Mutch NJ, Moore NR, Mattsson C, Jonasson H, Green AR, Booth NA. The use of the Chandler loop to examine the interaction potential of NXY-059 on the thrombolytic properties of rtPA on human thrombi *in vitro*. *Br J Pharmacol*. 2008;153(1):124-131.
21. Colucci M, Binetti BM, Tripodi A, Chantarangkul V, Semeraro N. Hyperprothrombinemia associated with prothrombin G20210A mutation inhibits plasma fibrinolysis through a TAFI-mediated mechanism. *Blood*. 2004;103(6):2157-2161.
22. Li W, Nieman M, Sen Gupta A. Ferric chloride-induced murine thrombosis Models. *J Vis Exp*. 2016;(115):1-12.
23. Dobrina A, Pausa M, Fischetti F, et al. Cytolytically inactive terminal complement complex causes transendothelial migration of polymorphonuclear leukocytes *in vitro* and *in vivo*. *Blood*. 2002;99(1):185-192.
24. Smith-Jackson K, Yang Y, Denton H, et al. Hyperfunctional complement C3 promotes C5-dependent atypical hemolytic uremic syndrome in mice. *J Clin Invest*. 2019;129(3):1061-1075.
25. Capolla S, Mezzaroba N, Zorzet S, et al. A new approach for the treatment of CLL using chlorambucil/hydroxychloroquine-loaded anti-CD20 nanoparticles. *Nano Research*. 2016;9:537-548.
26. Colombo F, Durigutto P, De Maso L, et al. Targeting CD34(+) cells of the inflamed synovial endothelium by guided nanoparticles for the treatment of rheumatoid arthritis. *J Autoimmun*. 2019;103(2019):102288-102301.
27. Macor P, Secco E, Mezzaroba N, et al. Bispecific antibodies targeting tumor-associated antigens and neutralizing

- complement regulators increase the efficacy of antibody-based immunotherapy in mice. *Leukemia*. 2015;29(2):406-414.
28. Mezzaroba N, Zorzet S, Secco E, et al. New potential therapeutic approach for the treatment of B-cell malignancies using chlorambucil/hydroxychloroquine-loaded anti-CD20 nanoparticles. *PLoS One*. 2013;8(9):E74216.
29. Cavalli R, Argenziano M, Vigna E, et al. Preparation and in vitro characterization of chitosan nanobubbles as theranostic agents. *Colloids Surf B Biointerfaces*. 2015;129(1):39-46.
30. Xing Z, Wang J, Ke H, et al. The fabrication of novel nanobubble ultrasound contrast agent for potential tumor imaging. *Nanotechnology*. 2010;21(14):145607-145615.
31. Argenziano M, Occhipinti S, Scomparin A, et al. Exploring chitosan-shelled nanobubbles to improve HER2 + immunotherapy via dendritic cell targeting. *Drug Deliv Transl Res*. 2022;12(8):2007-2018.
32. Marano F, Frairia R, Rinella L, et al. Combining doxorubicin-nanobubbles and shockwaves for anaplastic thyroid cancer treatment: preclinical study in a xenograft mouse model. *Endocr Relat Cancer*. 2017;24(6):275-286.
33. Shen S, Li Y, Xiao Y, et al. Folate-conjugated nanobubbles selectively target and kill cancer cells via ultrasound-triggered intracellular explosion. *Biomaterials*. 2018;181(1):293-306.
34. Cavalli R, Bisazza A, Lembo D. Micro- and nanobubbles: a versatile non-viral platform for gene delivery. *Int J Pharm*. 2013;456(2):437-445.
35. Brown T. Design thinking. *Harv Bus Rev*. 2008;86(6):84-92.
36. Cavalli R, Soster M, Argenziano M. Nanobubbles: a promising efficient tool for therapeutic delivery. *Ther Deliv*. 2016;7(2):117-138.
37. McCarthy JR, Patel P, Botnaru I, Haghayeghi P, Weissleder R, Jaffer FA. Multimodal nanoagents for the detection of intravascular thrombi. *Bioconjug Chem*. 2009;20(6):1251-1255.
38. Marsh JN, Hu G, Scott MJ, et al. A fibrin-specific thrombolytic nanomedicine approach to acute ischemic stroke. *Nanomedicine (Lond)*. 2011;6(4):605-615.
39. Alonso A, Dempfle CE, Della Martina A, et al. In vivo clot lysis of human thrombus with intravenous abciximab immunobubbles and ultrasound. *Thromb Res*. 2009;124(1):70-74.
40. Wang X, Palasubramaniam J, Gkanatsas Y, et al. Towards effective and safe thrombolysis and thromboprophylaxis: preclinical testing of a novel antibody-targeted recombinant plasminogen activator directed against activated platelets. *Circ Res*. 2014;114(7):1083-1093.
41. Hua X, Zhou L, Liu P, et al. In vivo thrombolysis with targeted microbubbles loading tissue plasminogen activator in a rabbit femoral artery thrombus model. *J Thromb Thrombolysis*. 2014;38(1):57-64.
42. Del Papa N, Sheng YH, Raschi E, et al. Human beta 2-glycoprotein I binds to endothelial cells through a cluster of lysine residues that are critical for anionic phospholipid binding and offers epitopes for anti-beta 2-glycoprotein I antibodies. *J Immunol*. 1998;160(11):5572-5578.
43. Lonati PA, Scavone M, Gerosa M, et al. Blood cell-bound C4d as a marker of complement activation in patients with the antiphospholipid Syndrome. *Front Immunol*. 2019;10(1):773-781.
44. Shantsila E, Lip GY. The role of monocytes in thrombotic disorders. Insights from tissue factor, monocyte-platelet aggregates and novel mechanisms. *Thromb Haemost*. 2009;102(5):916-924.
45. McCarthy JR, Sazonova IY, Erdem SS, et al. Multifunctional nanoagent for thrombus-targeted fibrinolytic therapy. *Nanomedicine (Lond)*. 2012;7(7):1017-1028.
46. Schwarz M, Meade G, Stoll P, et al. Conformation-specific blockade of the integrin GPIIb/IIIa: a novel antiplatelet strategy that selectively targets activated platelets. *Circ Res*. 2006;99(1):25-33.
47. Wang X, Gkanatsas Y, Palasubramaniam J, et al. Thrombus-targeted theranostic microbubbles: a new technology towards concurrent rapid ultrasound diagnosis and bleeding-free fibrinolytic treatment of thrombosis. *Theranostics*. 2016;6(5):726-738.